Available online at www.sciencedirect.com

ScienceDirect

Advances in Space Research 60 (2017) 999–1014

ADVANCES IN SPACE RESEARCH (a COSPAR publication)

www.elsevier.com/locate/asr

Equinoctial asymmetry in ionosphere over Indian region during 2006–2013 using COSMIC measurements

Malini Aggarwal [a,*], Ananna Bardhan [b], D.K. Sharma [b]

[a] *Indian Institute of Geomagnetism, New Panvel, Mumbai, India*
[b] *Department of Physics, Manav Rachna University, Faridabad, India*

Received 6 November 2016; received in revised form 2 May 2017; accepted 18 May 2017
Available online 25 May 2017

Abstract

In this study, the ionospheric equinoctial asymmetry (EA, defined as different ionospheric behaviour in the two equinoxes) is investigated in the maximum electron density (NmF2) and the corresponding altitude (hmF2) over the Indian region (~5–30° N geog. lat., 60–100° E geog. long.) during quiet geomagnetic conditions ($Ap \leq 20$) and varying phase of solar activity (2006–2013, F10.7 ~65–192 sfu) using COSMIC observations. Both NmF2 and hmF2 exhibited strong solar-activity dependence and which increased with the increase in solar activity throughout the day. We found EA in NmF2 is not just a daytime phenomenon but also occurs in morning and nighttime during high solar-activity. The EA in NmF2 over equatorial-low latitude is found solar-dependant in nighttime and morning (weaker/stronger in low-/high-solar activity) whereas stronger/weaker in noontime in low-/high-solar activity years (higher NmF2 in vernal in 2007–2009, 2013) respectively. Whereas for hmF2, EA is stronger in nighttime and weaker in morning for all years over both equatorial and low-latitudinal regions and weaker/moderate in low-/high-solar activity for noontime respectively. We found F10.7P and Dst index in the equinoxes playing a dominant role throughout the day and the chemical compositions (O, N_2 and neutral mass densities) also a responsible factor for the EA in NmF2 and hmF2 in the morning and nighttime respectively.

Keywords: hmF2; NmF2; Equinoctial asymmetry; COSMIC

1. Introduction

The earth's ionosphere is the ionized region of the upper atmosphere where sufficient number of free electrons exist to significantly affect the propagation of radio waves. The ionosphere can be affected by a variety of disturbances including, for example, solar disturbances, geomagnetic storms, severe weather, volcanoes, and earthquakes which can affect a variety of ground-based and space-borne technological systems (e.g. Davies, 1990; Hargreaves, 1995; Feynman and Gabriel, 2000; Aggarwal et al., 2012, 2013; Aggarwal, 2015). The uppermost region of ionosphere: F2 (>150 km) represents the maximum electron density and is a region of significant interest for radio propagation, exhibiting a variable characteristics and hence making it the most anomalous and a difficult region to predict. Ionospheric variability or deviation from climatological means is considered a permanent feature of the ionosphere which varies with local time, day-to-day, season and solar activities respectively (eg. Zhang and Holt, 2008; Sharma et al., 2005; Aggarwal et al., 2007). Under extreme geophysical conditions, sudden ionospheric changes may even cause serious threat to communication and navigation systems (Basu et al., 2002). As a result, a proper understanding of ionospheric variability such as, characteristics, causative processes, and prediction has become important for the aeronomy scientific community.

* Corresponding author.
E-mail address: asmalini@rediffmail.com (M. Aggarwal).

http://dx.doi.org/10.1016/j.asr.2017.05.020
0273-1177/

In terms of theory of Chapman (1931), which is based on the electron densities varying regularly with solar zenith angles in the ionosphere, the F2 region is anomalous in many ways and three major anomalies: seasonal, semi-annual and equinoctial asymmetry (EA) have been known to exist. The seasonal anomaly is the maximum/minimum electron densities in the winter/summer solstice respectively being contrary to the solar zenith angle variation (Croom et al., 1960) and has been inferred in terms of the thermospheric composition change caused by the prevailing upwelling/downwelling of molecular/atomic rich air in the summer/winter hemisphere respectively (e.g., Richards and Torr, 1986; Fuller-Rowell et al., 1988; Rishbeth et al., 2000; Pavlov and Pavlova, 2005). The semi-annual variability is the higher electron densities around the equinoxes and lower in solstices (Titheridge, 1973) and is caused by the variations of the neutral circulation in the thermosphere-ionosphere system which changes the ratio between atomic oxygen and molecular nitrogen concentrations (O/N_2) (Rishbeth et al., 2000). The annual/semiannual components in daytime electron density (Ne) for low solar activity in 200–560 km altitude exhibits a distinct latitudinal and altitudinal dependences and wave-like longitudinal structure (Liu et al., 2009). The third anomaly is the equinoctial asymmetry (EA), where solar zenith angle and solar activity conditions are almost similar in both vernal and autumn equinoxes, still differences exist in the ionospheric behaviour in the two equinoxes (Balan et al., 1998; Bailey et al., 2000; Kawamura et al., 2002; Chen et al., 2009; Aggarwal et al., 2012; Bardhan et al., 2014). The EA may be considered as a manifestation of the annual variation and occurs when the annual phase drastically shifts from the solstices (Liu et al., 2010a). The cause of the EA is believed as the effect of different parameters such as unequal solar flux, neutral composition such as $[O]/[N_2]$, electric fields, and thermospheric neutral wind velocities (Balan et al., 2000; Kawamura et al., 2002; Liu et al., 2003; Maruyama et al., 2009; Ren et al., 2011; Aggarwal et al., 2012). As extensive studies are mainly focused on the understanding of the physical processes of the annual and semiannual components but lesser towards the EA phenomenon, hence our interest here is to explore more the ionospheric EA using ionospheric parameters over equatorial-low latitude respectively.

Some of the results on ionospheric EA have been reported by the previous investigators using various ionospheric parameters. Da Rosa et al. (1973) using daily mean of TEC over Stanford (37.4°N, 122.2°W) between 1964 and 1971 found a higher peak for vernal than autumn during high as well as moderate solar activity period. Wan et al. (2008) observed EA in longitudinal wave number 4 structures; the wave is found to be stronger in northern autumn than in vernal. Balan et al. (1998) using MU radar found altitudinal dependence of EA being stronger at higher altitude. They found electron density (Ne) at lower/higher altitudes (lower/higher than ionospheric peak) to be slightly higher/lower in autumn than vernal respectively and Ne exceeded by 100% in vernal than autumn at higher altitudes. The field-aligned and field-perpendicular plasma velocities in the ionosphere and neutral wind and compositions in the thermosphere were found different in the equinoxes. The meridional component of the daytime poleward wind velocity derived from the field-parallel plasma velocity and O/N_2 from the MSIS model were found weaker in March than September equinox. Using Hinotori satellite (~600 km) measurements, Bailey et al. (2000) reported asymmetry in topside Ne at low latitudes to be hemispheric dependent (higher Ne in March/September in Northern/Southern hemisphere) and became more pronounced with increasing latitude in both hemispheres respectively. They suggested the mechanism to be the north-south imbalance of the thermosphere and ionosphere at the equinoxes due to slow response of the thermosphere arising from the effects of the global thermospheric circulation as found using CTIP model. According to Kawamura et al. (2002), the neutral wind velocities in the two equinoxes are found to be highly unequal or asymmetric, the direct effect of the neutral wind occurred through the changes in ionospheric height was opposite to the indirect effect of the wind which occurred through the changes in thermospheric composition. This caused a stronger EA in the ionosphere with Ne near and above the ionospheric peak being much stronger in March compared to September equinox, by over 100%. The asymmetry in the wind velocity is accounted for a weak asymmetry observed in the thermospheric composition and suggested the EA in the neutral wind velocity as due to the differences in the momentum/energy being transmitted from lower to upper atmosphere through tides and waves. The ionospheric parameters also changes in accordance with solar cycle variations (Aggarwal et al., 2007; Chen and Liu, 2010). During solar minimum period, Liu et al. (2010a) using COSMIC radio occultation, TOPEX, Jason-1, GPS and ionosonde measurements reported higher difference in equinoctial TEC and NmF2 (peak electron density) in low latitudes in both the hemispheres but lesser significant differences at the higher latitudes. They also found EA in hmF2 at low-latitudes indicating the difference in the neutral winds at the low latitudes in the equinoxes. Using TEC and ionosonde NmF2 data, Chen et al. (2012) found solar activity dependence, with increase in solar activity, EA of noontime NmF2 increased in mid-latitudes but decreased at low-latitudes, whereas EA in TEC increased at all latitudes. Recent observations by Liu et al. (2011) of the mean NmF2 around 1300 LT of the COSMIC measurements found higher NmF2 in March than in September equinox, and the EA was strongest over equatorial anomaly crest (~geog. 10-15°N) regions during year 2008–2009 respectively. Recent observations of EA over Indian subcontinent also have been reported by Aggarwal et al. (2012) and Bardhan et al. (2014). Aggarwal et al. (2012) during solar minimum period over Indian anomaly regions found strength of noontime equatorial ionization anomaly (Ic) exhibiting EA in GPS-TEC measurements with slightly higher values in spring (∼50 TECU) than autumn equinox (∼48 TECU). Bardhan et al. (2014) using SROSS C2 satellite measurements (∼500 km altitude) found strong EA in ionospheric plasma temperatures (electron, Te and ion, Ti) during early morning and daytime which decreases with increase in solar activity and disappearance/weaker EA existed during the nighttime in low/high solar activity respectively. Similar to Te and Ti, a decrease in EA in atomic oxygen ion densities (O^+) with solar activity during daytime is found. Considering, EA as a stronger phenomenon in low-latitudes, we focused our study on the characteristics of EA over equatorial and low latitude regions of Indian subcontinent using significant ionospheric parameters: maximum electron density (NmF2) and the corresponding altitude (hmF2) during geomagnetic quiet time during different levels of solar activity and to investigate whether EA is only a noontime phenomenon. For this, we obtained the NmF2 and hmF2 from COSMIC measurements over Indian region using complete 8 years of data during mission period for varying solar activity. Here the Section 2 gives the data used with Results and Discussion in Section 3 and summary in section 4 respectively.

2. Data used

To examine the prevailing background conditions during the study period, the daily solar flux index: F10.7 and geomagnetic indices: Kp (3-hourly), Dst (hourly) and Ap (daily) are obtained from OMNI website along with the daily solar EUV fluxes in both 26–34 nm and 0.1–50 nm energy bands from the SEM instrument aboard SOHO satellite (Judge et al., 1998, http://www.usc.edu/dept/space_science/) respectively. The F10.7 index (in terms of solar flux units, $1\ \text{sfu} = 10^{-22}\ \text{W/m}^2/\text{Hz}$) is based on measurements of the solar radio emission at the 10.7 cm wavelength, and has been widely used in past as a proxy of solar extreme ultraviolet (EUV) and lyman-α irradiances (Richards et al., 1994a; Tobiska et al., 2000). We considered a solar proxy, $F10.7P = (F10.7 + F10.7A)/2$, where F10.7A is the 81-day mean of daily F10.7 and F10.7P is believed to be a better proxy in a statistical sense as represents the intensity of solar EUV fluxes fairly well (Liu et al., 2006). As the electron production in ionosphere is maximum by the solar wavelength 0.1–50 nm which also produces O^+ (Richards et al., 1994a,b), hence this EUV band is considered a good indicator and is used hereafter. The existing background neutral atmosphere: O, O_2, N_2 number densities, O/N_2, O/O_2 ratios of number densities and total mass densities have been obtained using empirical MSISE-00 model (http://ccmc.gsfc.nasa.gov/modelweb/atmos/nrlmsise00.html).

For the ionospheric measurements, COSMIC (Constellation observing system for meteorology, Ionosphere and Climate/Formosat-3) satellite measurements (6 microsatellites, circular orbit, ∼512 km altitude and 72° inclination) are obtained using radio occultation (RO) payload. Later, the satellite altitude was raised to ∼700–800 km respectively. The RO technique has the advantages of limb sounding geometry, global coverage, and high vertical resolution in comparison with traditional ionospheric monitoring methods. The COSMIC RO measurements and products were obtained using the COSMIC Data Analysis and Archive Center (CDAAC, http://cdaac-www.cosmic.ucar.edu/cdaac/index.html) and we used the second level data "ionprf" files which includes information about ionospheric electron density profiles (EDPs). At CDAAC, the ionospheric electron density profiles are retrieved by using the Abel inversion technique from TEC along LEO–GPS rays (Schreiner et al., 1999; Syndergaard et al., 2006). The Abel inversion is used with several assumptions/approximations such as (i) straight line signal propagation, (ii) spherical symmetry of electron density profiles, (iii) circular satellite orbits, and (iv) first-order estimation of the electron density at the top (Kuo et al., 2004; Syndergaard et al., 2006). Among all the assumptions, the considered main source of inversion error is the spherical symmetry approximation in the horizontal direction (Tsai et al., 2001; Tsai and Tsai, 2004; Liu et al., 2010; Yue et al., 2010). Meanwhile, several studies examined the accuracy of the retrieved GPS/MET electron density profiles and found that the spherical symmetry assumption required for the Abel inversion introduces errors (Schreiner et al., 1999; Tsai et al., 2001; Tsai and Tsai, 2004). An error analysis obtained by Yue et al. (2010) on comparing the COSMIC electron densities (Ne) profiles with the NeQuick model found that the Abel inversion method introduces significant errors in the electron densities in low-latitude region. The assumption of spherical symmetry is not fulfilled at low latitudes where Ne exhibits strong horizontal gradients whereas small errors are observed for all altitudes at mid- and high-latitudes. The relative standard deviations of the differences between the determined and true values were 16% and 15% for NmF2, and 2% for hmF2 during both nighttime and daytime, respectively indicating a good agreement of the determined values of NmF2 and hmF2 but degrading at the lower altitudes. To avoid much error, we analyzed the data manually for some orbits to fix and removed the bad data points for electron density profiles with large, irregular spikes and data gaps. The data set includes about 2000–2500 vertical electron density profiles spread over globally in 1 day. Considering these factors for our study of interest, we determined the maximum electron density (NmF2) and the corresponding altitude (hmF2) from each occultation orbit for equinoxes over nearly Indian sector (∼5–30°N geog. latitude and ∼60–100° E geog. longitude) respectively. The data has been grouped in the two equinoxes: vernal and autumn. For vernal, March and April months and for autumn, September and October months have been considered for each year respectively.

3. Results and discussion

Fig. 1 represents the variability of daily solar fluxes: F10.7, EUV (26–34 nm and 0.1–50 nm) and geomagnetic indices: Ap during the year 2006–2013 respectively. The day-to-day variability of F10.7 ranged from 65 to 192 sfu and EUV flux exhibited trend similar to F10.7 ranging between 1.67×10^{10} ph/cm^2/s and 9.95×10^{10} ph/cm^2/s in 0.1–50 nm respectively. The similar trend is followed in 26–34 nm but with lower flux than 0.1–50 nm respectively. The annual F10.7 was slightly higher in year 2006 (∼80 sfu) than 2007–2009 (∼69–73 sfu) and then increases from 2010 to 2013 (∼80–122 sfu) and we considered period as low solar activity (LSA) during 2006–2010 and high solar activity (HSA) in 2011–2013 with highest values in 2013 respectively. The daily Ap indices were high on some days (upto ∼94) indicating the geomagnetic disturbed period on a few days (Fig. 1(b)). The dashed-line represents a separation line (Ap = 20) above which are the disturbed days and below represents the quiet days (low Ap ≤ 20) and the quiet days are only considered in our further study. The last panel in Fig. 1 represents the number of quiet days (left y-axis) for which the data has been incorporated and the averaged F10.7P (right y-axis) during each equinox of the year respectively. The number of days of data availability is higher (∼55) in each equinox for all years except the vernal, 2006 (∼5 days) as the COSMIC was launched in mid of month April, 2006. The averaged F10.7P (Fig. 1(c)) varied between 67 and 140 sfu during the equinoxes of 2006–2013 and is highest (∼140 sfu) in autumn, 2011 respectively. The F10.7P is slightly higher in vernal equinox than autumn during 2006–2008 and 2013 but values are slightly higher in other years in autumn. And hence the difference between the two equinoxes in each year is negligible during LSA and HSA period but is higher during years 2011 and 2013 respectively. However, the differences of yearly averaged ionospheric parameters in vernal and autumn should not be significantly affected by the variations in solar activity as the difference in F10.7P between the two equinoxes is lesser (higher/lower in vernal in LSA/HSA).

To illustrate the method used to obtain the NmF2 and hmF2 values, we represented in Fig. 2, an example of COSMIC observations for the considered Indian longitude sector on two quiet days (vernal: 18 Apr 2007, first row and autumn: 1 Sep 2007, second row) having similar EUV fluxes (∼1.95×10^{10} ph/cm^2/s) respectively. The orbital occultation paths for different UT (shown by filled-coloured symbol) for each COSMIC satellites (17 orbits on 18 April and 20 on 1 Sep) are shown in the left panels (Fig. 2(a) and (d)) respectively. The electron densities

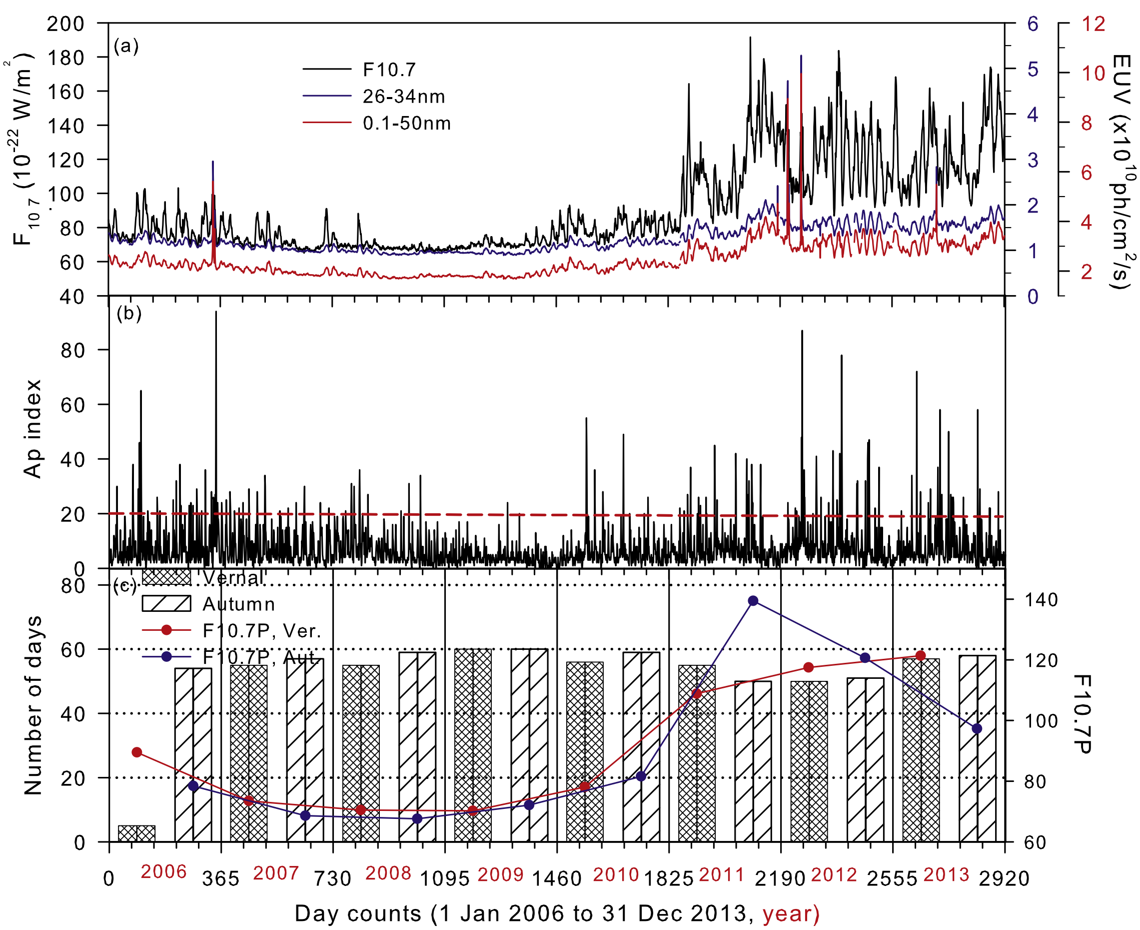

Fig. 1. Variability of (a) solar flux: F10.7 (left-axis) and EUV flux (right-axis) in 26–34 and 0.1–50 nm, (b) geomagnetic indices, Ap and (c) number of quiet days and averaged F10.7P considered during vernal and autumn equinoxes of during year 2006–2013 respectively. The dash line in (b) represents the quiet magnetic activity period (Ap < =20).

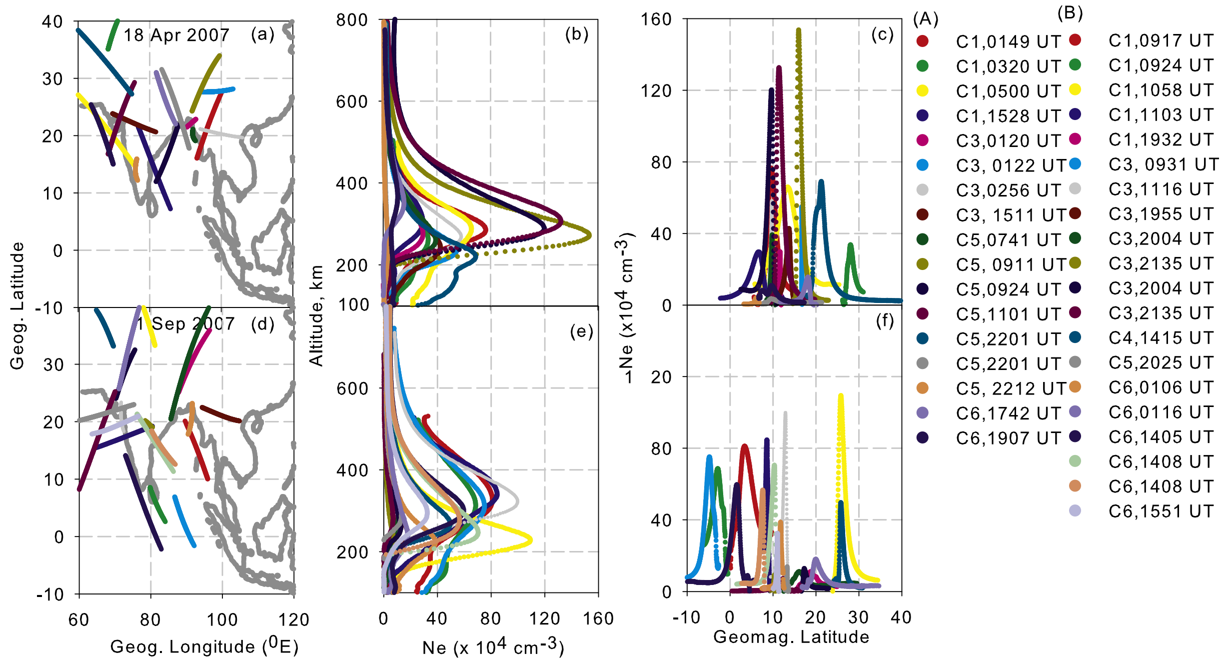

Fig. 2. Representation of COSMIC observations as an example on vernal (18 Apr 2007, first row) and autumn (1 Sep 2007, second row) day respectively. Shows the (a) COSMIC occultation orbital paths over Indian longitude sector, (b) electron density profiles varying with altitude and (c) electron density varying with latitude on a quiet day of 18 Apr 2007 in vernal equinox. (Second row) Same as first row but for 1 Sep 2007 respectively. The legend (A) is for 18 Apr and (B) for 1 Sep 2007 representing the pass-time (UT) of the COSMIC satellite respectively.

varying with altitude (electron density profiles, EDPs) for each orbit is shown in the middle panel from which the peak electron density, NmF2 and the corresponding altitude, hmF2 are obtained for each orbit (Fig. 2 (b) and (e)). The latitudinal variation of the electron density for the orbits are shown in the last column (Fig. 2 (c) and (f)). We observed the hmF2 varying around ∼200–300 km altitude on vernal (Fig. 2(b)) and ∼250–350 km on autumn day (Fig. 2(e)) respectively. The maximum value of NmF2 is $\sim 1.5{}^{*}10^{6}\ \mathrm{cm}^{-3}$ and $\sim 1.0{}^{*}10^{6}\ \mathrm{cm}^{-3}$ as found from the different orbits on 18 April 2007 and 1 Sep 2007 respectively. We found here noticeable differences in the equinoxes for NmF2 and hmF2 values which in general is also a function of the local time and latitude respectively.

3.1. Variability of NmF2 parameter in equinoxes

As the ionospheric behaviour over equatorial and low-latitude region is different, we separated the ionospheric parameters for equatorial (geog. ∼5°–10°N) and low-latitude (geog. ∼10°–30°N) respectively. The quantitative day-to-day variability of ionospheric parameters is defined by the coefficient of variability (CV) statistically as

$$CV\ (\%) = \frac{\sigma}{M} * 100 \tag{1}$$

Here the CV for NmF2/hmF2 describes the extent of spread of standard-deviation (σ) of hourly NmF2/hmF2 from the hourly mean (M) for the entire data set (Bilitza et al., 2004).

Fig. 3 represents the diurnal variability of hourly mean NmF2 and CV for the equatorial (Fig. 3(a) and (b)) and low-latitude (Fig. 3(c) and (d)) during each year for both vernal and autumn equinox respectively. The NmF2 at a location is actually the integrated effect of production (mainly controlled by solar radiation), loss (charge exchange with neutrals) and transport processes (dominated by equatorial fountain effect). The NmF2 is lowest throughout the nighttime which start increasing in early morning during sunrise when the photoelectron production also initiates and becomes a maximum in noontime and then decreases in nighttime as a result of competitive effects of absence of photo-ionization and occurrence of higher recombination rate of electrons with neutrals and ions. The NmF2 increases with rising solar activity (2006–2013), a higher increase is observed throughout the day from year 2006 (peak in noontime $\sim 1 \times 10^{6}\ \mathrm{cm}^{-3}$) to 2013 (noontime $\sim 1.5 \times 10^{6}\ \mathrm{cm}^{-3}$) with lesser differences in both equinoxes during nighttime but more in daytime respectively.

Over equator (Fig. 3(a)), the vernal NmF2 increases rapidly in morning, peaks earlier (∼1 h) and then decreases faster in the evening than in the autumn equinox indicating a faster response in vernal of the electron-production in the morning and recombination in the evening respectively. The noontime peak in NmF2 shows a clear solar activity dependence, being highest in HSA period (2011–2013) for both the equinoxes and regions respectively. On comparing the NmF2 values over equatorial and low-latitude regions, we found lesser difference in nighttime during all

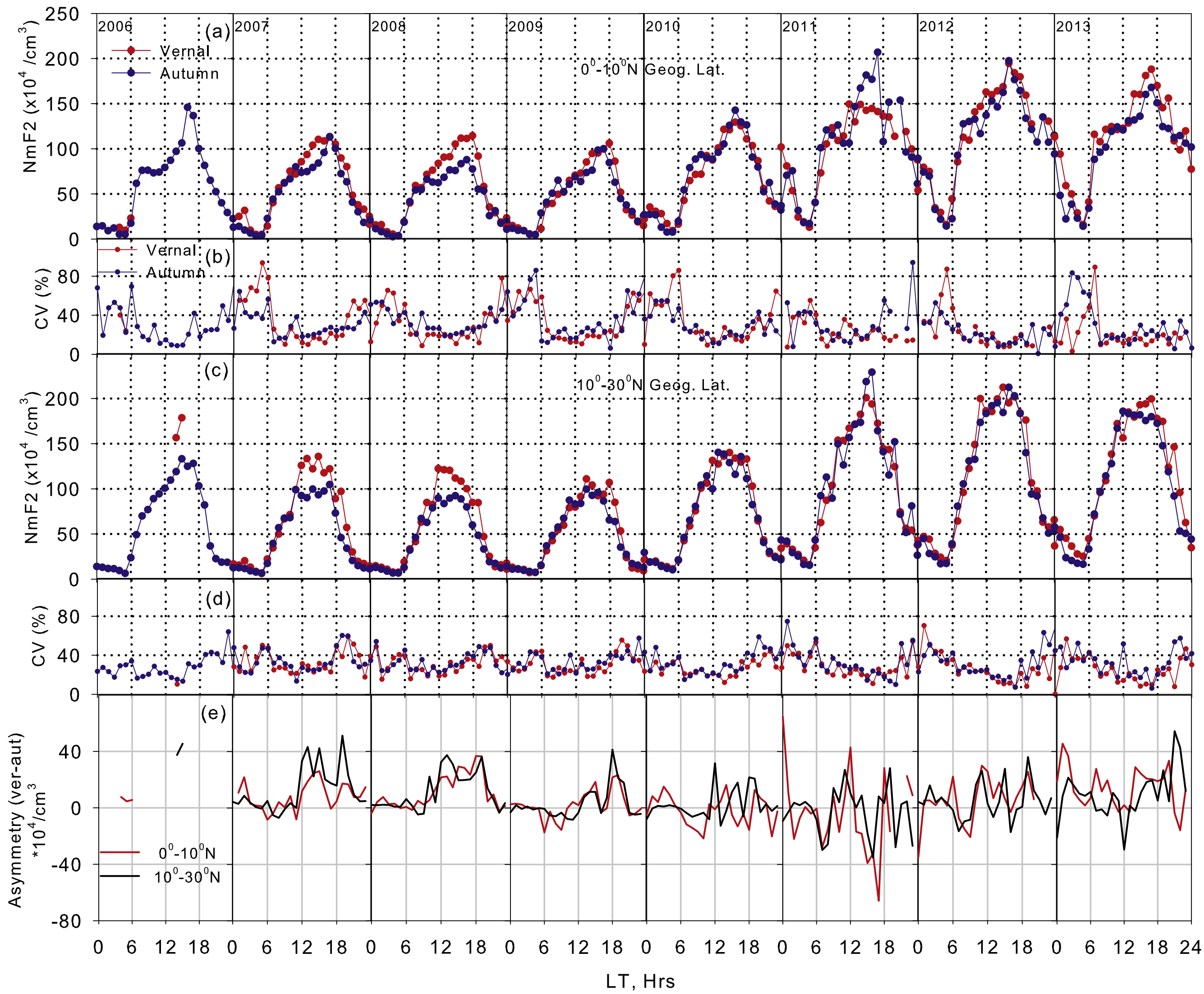

Fig. 3. Variability of hourly mean and standard deviation of NmF2 with local time during vernal and autumn equinoxes over 0°–10°N ((a) and (b)) and 10°–30°N ((c) and (d)) geographic latitude during year 2006–2013 respectively. The difference in the equinoxes is represented as an asymmetry and is shown in (e).

solar activity periods and noontime in LSA (2007–2010) but NmF2 is higher in noontime over low-latitude than equatorial region during HSA period indicating an existence of stronger equatorial ionization anomaly (EIA) during HSA period respectively. This is in agreement to Huang and Cheng (1996) of a stronger EIA in TEC in Asian sector during high solar activity period. The EIA phenomenon exhibiting a minima in electron density (Ne) near the dip equator and the two maximas in low-latitude on both side of the equator has been attributed to a fountain effect mainly driven by the large-scale eastward electric field at low latitudes (e.g., Abdu et al., 1990; Rishbeth, 2000). An evening enhancement (1800–1900 LT) in NmF2 is observed over equator during HSA (2011–2013) and over low-latitude during 2009–2013 and a post-midnight enhancement (0000-0300 LT) over both the regions during 2010–2013 respectively. This enhancement occurs due to the pre-reversal enhancement (PRE) of eastward electric field which at times occurs during sunset and then the plasma is lifted upward by EXB drift where loss rate also reduces. According to Abdu et al. (2010), the PRE variabilities can arise from various sources: (1) upward propagating planetary waves (Abdu et al., 2006), (2) prompt penetrating and disturbance dynamo electric fields (Abdu, 1997; Fejer and Scherliess, 1997), (3) disturbance winds during magnetic storms (Abdu et al., 1995) and (4) variability in the solar flux (F10.7) (Fejer et al., 1991; Batista et al., 1996). As our study period is during geomagnetic quiet period, only solar flux control and upward propagating planetary waves of the PRE is of particular interest as it also effects the ambient ionospheric and thermospheric parameters that directly or indirectly contributes in the generation of the PRE.

The hourly CV in NmF2 during equinoxes (Fig. 3 (b) and (d)) is lower (≤40% for equatorial, ≤50% for low-latitude) during daytime but higher in nighttime and early morning hours (upto 90% for equatorial, 75% for low-latitude) irrespective of the solar activity respectively. The day-to-day variability in NmF2 at equatorial-low latitudes may be attributed to the daily changes in the sun's EUV flux, equatorial electrojet (EEJ) and the dynamics of the neutral winds (Rama Rao et al., 2006). The variability of mean NmF2 (or f0F2) during sunrise and sunset is due to the steep electron density gradients caused by the onset and turn-off of solar radiation (Bilitza et al., 2004; Chuo and Lee, 2008) and overlay of the ionospheric F-region irregularities (spread F) on the background electron densities as suggested by Woodman and La Hoz (1976). For American and European sector, Ezquer and Mosert (2007) found a higher f0F2 variability during low solar activity than in high-solar activity and was larger by night than day which is also in agreement to our COSMIC observations for the Indian sector but for NmF2 in both the solar activities. Similar results were revealed using f0F2 by Akala et al. (2010) during nighttime over Southeast Asian sector. Aravindan and Iyer (1990) for low solar activity over low-latitude stations also found lower variability in ionospheric electron content (IEC) (10–25%) in daytime and higher (30–40%) in nighttime for all considered stations with lowest (<15%) variability at equatorial region which increased to 26% near the crest of equatorial anomaly during daytime. We also found a slight higher variability for low-latitude than equatorial regions using COSMIC observations.

The last panel (Fig. 3(e)) represents the equinoctial asymmetry (EA, defined as different behaviour in the equinoxes) in NmF2 characterized as the difference of hourly vernal and autumn NmF2 (positive/negative values corresponding to higher/lower values in vernal than autumn equinox) respectively. As the data availability is lesser in vernal for year 2006, hence nothing can be said about the EA for year 2006. For both the latitudinal regions, the difference in the two equinoxes during nighttime (2000-0300 LT) is lower (upto $\sim 2.0 \times 10^5$ cm^{-3}) in LSA indicating a weaker EA in nighttime during LSA but the difference increases during HSA representing a stronger EA. Similar behaviour is observed during morning hours (0400-0800 LT) for both the regions and solar activities respectively. The noontime NmF2 (1200-1500 LT) over both the regions is higher in vernal in year 2007-2009 and 2013 and slightly-/very-higher in year 2010, 2012/2011 in autumn respectively. This indicates a stronger noontime EA during LSA period than HSA respectively and is recognized as slightly higher solar activity (F10.7 and EUV flux) in vernal in year 2006–2008 and 2013 leading to a higher production of electrons (higher NmF2) in vernal in these years (Fig. 1(a)). The EA in NmF2 during noontime is found stronger over low-latitude than equator from our observations which is in agreement to Liu et al., (2011).

3.2. Variability of hmF2 parameter in equinoxes

To understand the ionospheric behaviour in equinoxes, another important ionospheric parameter: altitude corresponding to NmF2, hmF2 is investigated which also provides the useful information from which the meridional winds may be deduced for understanding the background ionosphere and also for assessing the thermospheric general circulation models (e.g. Miller et al., 1986, 1997). The general diurnal trend of hmF2 over equatorial (Fig. 4(a)) and low latitudes (Fig. 4(c)) exhibits two maxima (noontime and evening/midnight) and two minima (early-morning and before-evening (~1700 LT)/before-midnight (~2200 LT)) and with a higher height over the equator throughout the day for both the equinoxes. The F2 layer rises gradually during morning (from ~0700 LT) onwards when photo-electron production also initiates, and a noontime peak occurs around 1400 LT after which the F-layer comes down to lower altitudes, reaching a minimum around evening hours (~1700-1900 LT). The hmF2 varied from ~220 to 500 km and ~215 to 355 km over the equator and low latitude throughout the day during 2006–2013 respectively. This higher variability in altitude at equatorial-low latitude is expected as the F-region gets elevated to higher altitudes at the equator due to stronger EEJ in the equinoxes and hence the increased EXB drift uplifts the plasma layer to higher altitudes. The noontime hmF2 represents a clear solar-activity dependence where hmF2 increased from ~320 to ~400 km and ~275 to ~350 km over equatorial and low latitude during year 2006–2013 respectively. Similar observations were found by Rama Rao et al. (2006) using ionosonde measurements for a very high solar activity year (cycle: 23, F10.7 ~181 sfu) of March 2001 over Indian region and found noontime hpF2 (~hmF2) to be much higher (~450 km) at equatorial region than at and beyond the anomaly crest regions (~325–450 km) owing to the higher F10.7 respectively.

Over the equator (Fig. 4(a)), the morning hmF2 for both equinoxes show a solar activity dependence where minimum of hmF2 layer height (in early-morning) increases with the increase in solar activity. The lower hmF2 during early morning hours is due to the rapid production of ionization in the lower F region during sunrise, the intensive ionization begins resulting in the increased electron concentration near the F2-peak at a rate which depends primarily upon the production rate (see, e.g. Rishbeth and Garriott, 1969). However similar to early increase in vernal NmF2 over equator (Fig. 3(a)), the vernal hmF2 layer also starts rising prior than autumn hmF2 in the morning hours (Fig. 4(a)). Another diurnal peak in hmF2 is observed during evening (in HSA, 2011–2013) and midnight in all years (2006–13). The post-sunset rise in hmF2 is lower/higher than noontime peak during LSA (2006–2010)/HSA (2011–2013, upto ~500 km) respectively. This occurs due to an enhanced vertical drift of F layer plasma produced by the increased zonal electric field, known as the evening pre-reversal enhancement (PRE) of electric field over the

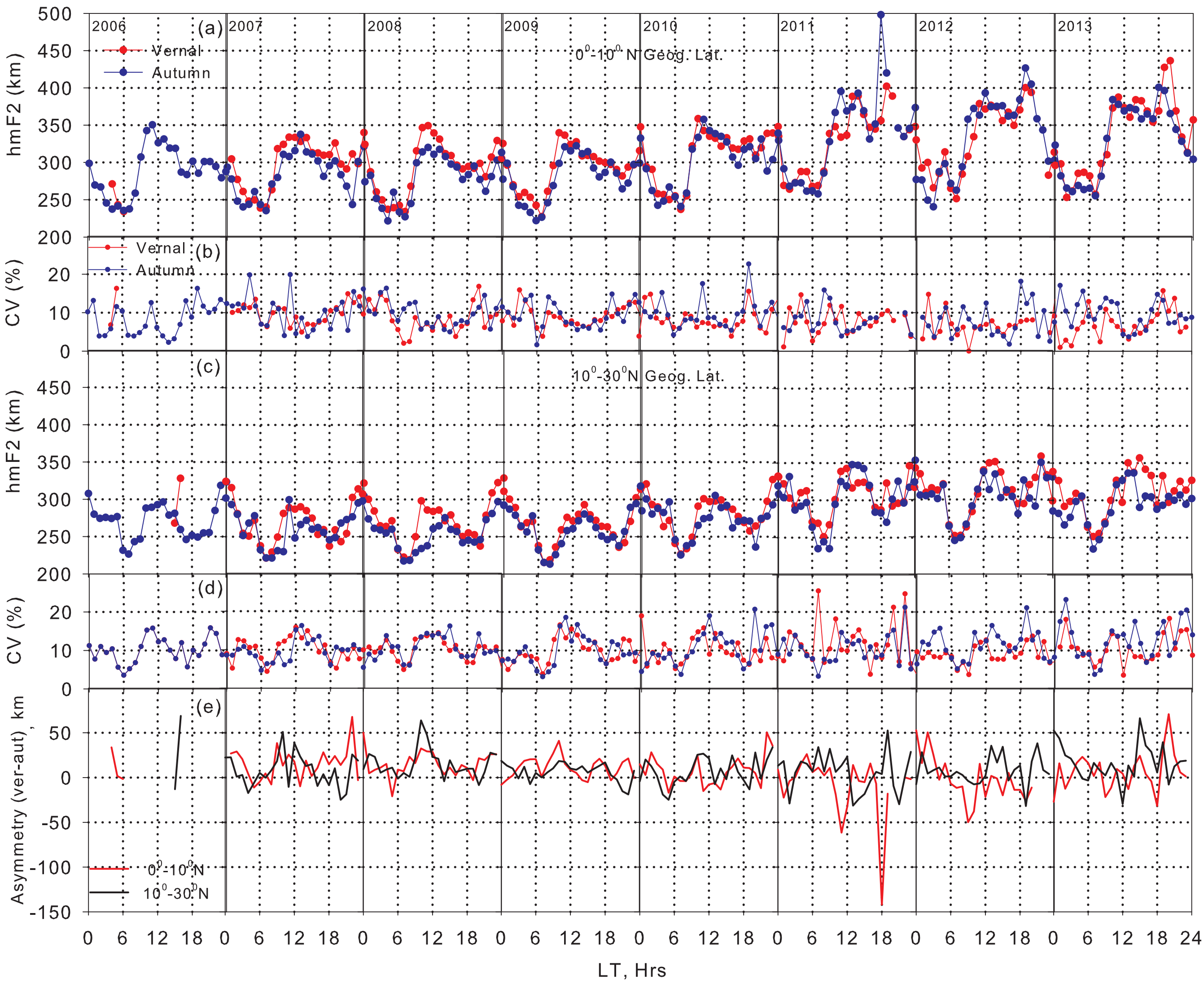

Fig. 4. Same as Figure-3 but for hmF2.

equator in the evening. In the evening as the rate of ion production ceases, an upward drift causes an additional uplift of the layer produced by a change in the direction of the thermospheric winds and hence increases the hmF2. During HSA, the uplift is even higher (upto ~500 km) as EXB is stronger leading to even higher hmF2 than noontime. The PRE vertical drift strongly depends on solar activity level and season and enhances with solar activity, and the increase is found stronger in equinoxes but weaker in summer (e.g., Fejer et al., 1991, 2008; Scherliess and Fejer, 1999). This increase in hmF2 is in accordance to the evening enhancement in NmF2 (Fig. 3). As the layer rises up, recombination rate decreases and increases the NmF2. We also observed post-midnight enhancement in hmF2 in all years which is a consequence of an increase of the upward drifts produced by the meridional winds in the neutral air (Hanson and Patterson, 1964; Kohl and King, 1967). In general, the F region equatorial electrodynamic plasma drifts are upward and westward during the daytime and downward and eastward in the nighttime having largest amplitudes around 0900 and 1100 LT (~25–30 m/s) (Scherliess and Fejer, 1999). The drift exhibit morning and evening reversals from downward nighttime to upward daytime and vice-versa in evening time respectively. During daytime, the temperature and atomic oxygen density and loss coefficient, which is proportional to the molecular component also increases, resulting in higher hmF2; accordingly, the rise of hmF2 from morning to afternoon is also due to enhanced temperature (Sethi et al., 2004). Over low-latitude (Fig. 4(c)), the rate of rise of noontime hmF2 with the solar activity is lower than over equator. A secondary enhancement in hmF2 during midnight for all solar activities which is even higher than noontime hmF2 for LSA but of similar height for HSA is observed which is distinct from the equatorial hmF2 variability. No post-sunset enhancement in hmF2 is observed over low-latitude region. We found a trend similar for both the equinoxes and regions but quantitative differences do exist.

The hourly CV in hmF2 (Fig. 4(c) and (d)) over the equator is higher in autumn (upto 22%) than vernal (upto 16%) during early morning and nighttime for both solar activities, whereas for low-latitudes is lower (upto 15%) in LSA but higher in HSA (25%) for both the equinoxes. In noontime, higher variability (CV) is observed in autumn (upto 20%) than vernal for both regions ($\sim$12% for equator and 15% for low latitude) and solar activities except year 2011 where CV is higher (upto 25%) in vernal for low-latitude respectively. The variability of hmF2 also gets affected by the equatorial $E \times B$ drift, as well as by thermospheric neutral winds. Sethi et al. (2004) for high solar activity year, 2001–2002 from a station, Delhi (28.6°N, 77.2°E) also found a large diurnal and day-to-day variability in ionosonde hmF2 during equinoxes which is in agreement with our COSMIC observations.

The EA in hmF2 defined similar to EA in NmF2 for both regions is represented in Fig. 4(e). During nighttime (2000-0300 LT) over the equator, hmF2 is higher in vernal for all years (upto $\sim$70 km) except 2011 (vernal hmF2 is lower) whereas for low-latitudes, lower/higher values are observed in vernal during pre-midnight (2000–2300, upto 30 km)/post-midnight hours (0000-0300 LT, $\sim$50 km) in hmF2 respectively indicating a stronger (over equator) to moderate (over low-latitude) EA in nighttime for both LSA and HSA respectively. During morning hours (0400-0800 LT), a weaker asymmetry in hmF2 is observed with $\pm$20 km difference over both the regions and solar activities. Whereas in noontime (1200–1500 LT), the difference in both equinoxes is lesser in LSA for both the regions whereas in HSA, vernal values are lower (upto 50 km and $\sim$140 km in year 2011) over equator and higher ($\sim$30 km) over low latitude indicating a moderate EA in hmF2 for HSA in noontime respectively.

3.3. Relation of NmF2 and hmF2 with background conditions in equinoxes

The ionization, recombination, and dynamic processes are significant for the formation of ionospheric F2 peak (e.g., Ivanov-Kholodny and Mikhailov, 1986; Rishbeth and Garriott, 1969); as not just the changes in solar EUV flux and X-ray radiations, but the neutral atmosphere and dynamical processes are also important for the daytime NmF2. As the neutral composition in the thermosphere also has a strong influence on electron density (Ne) in the upper ionosphere since the electron production rate depends on the atomic oxygen densities, O, whereas the loss on the molecular species N_2 and O_2 respectively. Hence increase in O/N_2 and O/O_2 increases the equilibrium electron density. Thus the existing background neutral concentrations in the equinoxes: O, O_2, N_2 number densities, O/N_2, O/O_2 ratios and total mass densities in g/cm^3 is obtained using MSISE-00 model at an altitude of mean COSMIC hmF2 observations for nighttime (2000-0300 LT), morning (0400-0800 LT) and noontime (1200-1500 LT) using F10.7P values for each equinox over both equatorial and low-latitude (0° and 20° N geog.) and 77°E longitude respectively. The general diurnal trend of O, O_2, N_2 number densities and mass densities exhibits a minimum during nighttime and increases in daytime (peak in noontime) whereas O/N_2 and O/O_2 exhibits a peak in morning and a minimum in noontime to evening respectively. We determined the association of ionospheric parameters (NmF2 and hmF2) with various factors: solar (F10.7P, EUV-1 (26–34 nm), EUV-2 (0.1–50 nm)), geomagnetic indices (Kp and Dst) and neutrals (O, O_2, N_2 number densities, O/N_2, O/O_2 ratios and total mass densities) as represented in Fig. 5 respectively to understand the relation of NmF2 and hmF2 with these factors.

We found (from Fig. 5(a)), an existence of a strong relation (0.8–1.0) of NmF2 with F10.7, EUV-1 and EUV-2 fluxes as expected (except being moderate in morning-vernal NmF2 over equator) throughout the day for both the equinoxes and regions (also from Fig. 3). For the whole day, the geomagnetic Kp index is found unrelated (<0.35) for both equinoxes whereas Dst is moderately anti-correlated ($\sim$0.5–0.7) in autumn over both the regions indicating a distinct role of hourly geomagnetic activity in the EA. Though O density during nighttime is weakly correlated with NmF2 but exhibited a different behaviour in equinoxes (positive/negative for vernal over equatorial/low-latitude and for autumn over low-latitude/equatorial region). During morning and noontime, O is found inversely moderate to strongly related (0.4–0.9) in both the equinoxes respectively. On the other hand, molecular compositions (O_2, N_2 and O/N_2) in the morning and noontime are found to be strongly correlated with NmF2 for both the equinoxes and regions whereas in nighttime are moderately correlated with NmF2 except being independant for equatorial-vernal (O_2, N_2, O/N_2) and low-latitude autumn (N_2, O/N_2) respectively (Note: O_2 and N_2 are anti-correlated with NmF2 and O/N_2 is directly correlated throughout the day). The ratio O/O_2 is found to associate moderate to strongly (0.64–0.96) with NmF2 throughout the day. The mass density very similar to O densities exhibits strong relation with NmF2 during morning and noontime but weaker in nighttime with a reversed relation observed in the equinoxes (direct-/anti-correlated in vernal/autumn for equator and reversed for low-latitude) respectively.

Similar to NmF2, hmF2 (Fig. 5(b)) for both the equinoxes is found to be strongly related with solar activity indices throughout the day (except moderate in noontime-vernal hmF2 over low-latitude) whereas Kp and Dst is independant except the Dst in autumn (moderate to strongly anti-related) for both the regions throughout the day. During nighttime, though NmF2 shows a weaker correlation with O densities, but the hmF2 moderately correlates with O densities for equatorial-autumn and low-latitude-vernal respectively. During other times of day

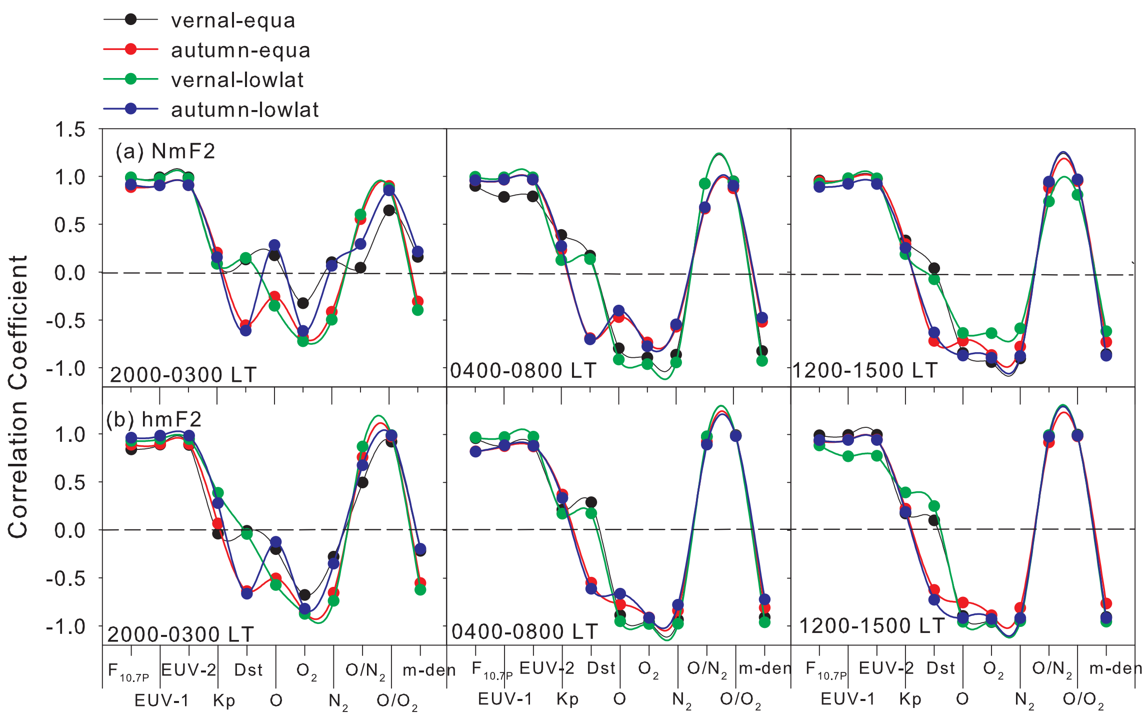

Fig. 5. Representation of the correlations of (a) NmF2 (first row) and (b) hmF2 (second row) with F10.7P, EUV-1 (26–34 nm), EUV-2 (0.1–50 nm), Kp, Dst, O, O_2, N_2, O/N_2, O/O_2 and total mass densities (m-den) over equatorial and low-latitude regions for both vernal and autumn equinoxes during nighttime (2000-0300 LT), morning hours (0400-0800 LT) and noontime (1200-1500 LT) respectively.

(morning and noontime), hmF2 strongly correlates with O densities similar to NmF2. The hmF2 exhibits strong relationship with O_2, O/O_2 and O/N_2 densities throughout the day for both the equinoxes, whereas hmF2 is independent of N_2 and mass density in nighttime for equatorial-vernal and low-latitude-autumn but is strongly related with hmF2 at other times of day and regions.

We found using COSMIC observations that both NmF2 and hmF2 over equatorial and low latitudinal regions demonstrates the general diurnal trend during the equinoxes in agreement to the previous ground based ionosonde measurements over Indian sector (Rama Rao et al., 2006; Sethi et al., 2004). Chu et al. (2010) on comparing the NmF2/hmF2 values by COSMIC and ground-based ionosondes found lower/higher values by COSMIC than ionosondes and the discrepancy in NmF2 was found latitude dependant, smaller in low and mid-latitudes but larger in high-latitude region. Whereas Krankowski et al. (2011) over European stations found COSMIC profiles to be in good agreement with ionosonde profiles in general, both in F2 layer, NmF2 and the bottomside profiles. Tsai et al. (2001) examined the electron density profiles from co-located GPS/MET and ionosonde measurements at mid latitude and at the EIA region and found that the GPS/MET overestimates foF2 at mid-latitude but underestimated in the EIA region. They suggested that an asymmetry of the EIA most likely causes the Abel inversion to systematically underestimate the electron density near the F2-peak. Liu et al. (2010b) compared the NmF2 and hmF2 using COSMIC and ground-based ionosonde observations at equatorial station, Jicamarca (12°S, 283° W) and found that in general COSMIC underestimated the NmF2 and hmF2 values. Under the assumption of the spherical symmetry which was not considered valid in the pronounced EIA regions, they found that at the geomagnetic equator the COSMIC overestimates NmF2 in the afternoon, underestimates the hmF2 in daytime, and overestimates the electron density under the F2-peak in daytime. On comparison of NmF2 and hmF2 ionospheric parameters at the equatorial latitude (Chu et al., 2010) and low latitudes (Straus, 2007; Wu et al., 2009) a better accuracy of RO measurements in NmF2 than hmF2 is indicated. The discrepancy between them is smaller in low- and mid-latitude and larger in high latitude regions (Chu et al., 2010). Hu et al. (2014) reported a decrease in the correlation between COSMIC and ionosonde measurements at high solar activity but with a higher correlation of NmF2/hmF2 during the nighttime/daytime respectively. Recent studies by Kumar et al. (2016) using different stations around the globe, found a stronger correlations of ionosonde and COSMIC NmF2 measurements during the equinoxes over equatorial (Jicamarca) and low-latitude station (Darwin) during daytime (0.88 and 0.72) and nighttime (0.96 and 0.95) respectively. Similar correlations for hmF2 is found over Jicamarca during the daytime (0.88) and nighttime (0.93) respectively. Recent studies over an Indian station, Dibrugarh (27.5°N, 95°E), Kalita and Bhuyan, 2017) found the COSMIC and ionosonde measured bottom side electron density profile are nearly same.

One of the striking new feature of ionospheric observations found using COSMIC measurements is the occurrence of strong equinoctial asymmetries (EA) in peak electron density (NmF2) in morning and nighttime in HSA alongwith noontime in all years (stronger in LSA) and the higher equinoctial differences in the corresponding altitude (hmF2) in nighttime during both solar activities and noontime in HSA over both latitudinal regions respectively. The previous studies on EA were mainly based on noontime features in electron densities (Ne), plasma temperatures, TEC, field-parallel and perpendicular plasma velocities and has been interpreted in terms of the corresponding asymmetries in the solar flux, thermospheric composition and neutral winds (for eg. Balan et al., 1997, 2000; Kawamura et al., 2002; Aggarwal et al., 2012; Bardhan et al., 2014). In the equinoxes, the subsolar point lies around the equator, where the eastward electrojet-associated electric field is also often strongest. Hence the fountain effect developed due to collocation of the peak photoelectron abundance and the intense eastward electric field region is also stronger (Wu et al., 2004). The ionospheric behaviour of EA in NmF2 is found similar over both the latitudinal regions and EA existed in nighttime and morning varying with solar activity (weaker/stronger in LSA/HSA) respectively. This is because the difference in F10.7P is lesser in the equinoxes during LSA but higher in years 2011, 2013 (Fig. 1(c)) which produces the higher and different electron densities in the noontime in the equinoxes and maintains the higher background in the nighttime and morning hours also in years 2011, 2013 respectively. In addition, Ren et al. (2011) found different equatorial $E \times B$ vertical drift in the F2 peak region at 600 km which induces the EA of the Ne at low latitudes. A higher $E \times B$ vertical drift in daytime will cause a stronger fountain effect affecting changes in the latitudinal distribution of the plasma density at low latitudes thereby moving the plasma from the equator to the low-latitude regions thereby the NmF2 decreases/increases over the equator/low-latitude respectively. Hence difference in the EXB vertical drift during equinoxes may also induce the EA in NmF2 over equator and low-latitude respectively. We found EA during noontime to be solar activity dependant and is stronger in LSA and weaker in HSA years (higher NmF2 in vernal for years 2007–2009 and 2013). One of the factor of higher NmF2 in vernal is because of higher production rate of electrons as F10.7P is slightly higher/lower in vernal in LSA (2006–2008)/HSA (2010–2012) than autumn except the year 2013 when F10.7P in vernal is higher and year 2009 when it is similar in both the equinoxes (Fig. 1(c)) respectively. The slightly higher F10.7P in vernal introduces a stronger EA (in LSA and 2013 year) but the HSA years in which F10.7P is higher in autumn, EA is not very strong (HSA) except year 2011. This indicates that factors other than F10.7P also plays a significant role in EA in NmF2 during daytime like equatorial electrojet (EEJ) and the neutral winds. Similar observations were previously reported over Indian anomaly region using GPS-TEC observations during daytime for solar minimum period by Aggarwal et al. (2012). Their observations showed the strength of equatorial ionization anomaly (Ic) exhibiting an asymmetrical semi-annual double peak with slightly higher amplitudes in spring (~50 TECU) than in autumn equinox (~48 TECU) respectively. Similar results were also obtained by Chakraborty and Hajra (2008) using TEC observations over Indian station and suggested the neutral wind as one cause which blows predominantly northward from October to April month, leading to a higher TEC values in vernal equinox. Unnikrishnan et al. (2002) from a far-away low latitude station, Palehua (19°N, 206°E) found opposite EAs in TEC between HSA and LSA with higher/lower TEC in September than March equinox during high-(year 1981)/low-(year 1984) solar activity and attributed it to the different solar activities in both equinoxes in a year respectively. Their results are in agreement to our observations where EA in NmF2 reverses with F10.7P, higher F10.7P in low/high solar activity produces higher NmF2 in vernal/autumn respectively. Chen et al. (2012) found opposite relation of NmF2 and TEC with solar activity and the NmF2/TEC decreases/increases with the increase in solar activity and considered the different ionospheric scale height in the equinoxes to be a cause for it as revealed by Liu et al. (2007). The rate of increase of ionospheric scale height with the solar P index is found higher in March than September equinox over Arecibo. This asymmetry in solar activity of the scale height suppressed the equinoctial difference in NmF2 increased rates which featured the higher increased rate in September than March and resulted in higher increase of TEC with P in March than in September equinox respectively.

We found latitudinal differences in EA for hmF2 during nighttime (2000-0300 LT), over equator a higher hmF2 (upto ~70 km) in vernal for all years except 2011 whereas over low-latitudes, the lower/higher F-layer in vernal than noontime during pre-/post-midnight hours is observed. As a result EA in nighttime hmF2 is found to be stronger/moderate over equator/low-latitude respectively. For both regions, a weaker EA in hmF2 is observed (±20 km) in morning hours but in noontime, a weaker EA in LSA occurs with lower (~50 km, upto 140% in year 2011)/higher (~30 km) over equator/low-latitude in vernal during HSA respectively generating a stronger EA in hmF2 in HSA during noontime. We observed different EA in hmF2 over equator and low latitude throughout the day. The influence of neutral winds on hmF2 is considered as dependant on sin(2I), where I is the geomagnetic dip (e.g. Rishbeth, 1972). Ren et al. (2011) during 0900-1300 LT found higher EXB plasma drift velocity (V⊥) in the equatorial F region at northern spring (March-April) than autumn (September-October) and suggested the asymmetry in MLT tides may play a significant role in the asymmetry of equatorial V⊥. An EA existed for wave number 4 longitudinal structures of V⊥ throughout the daytime and extended to the evening sector at autumn equinox, while appearing mainly at noon and pre-noon at spring equinox. They observed an asymmetry of the pre-reversal enhancement (PRE) in sunset occurring with maximum PRE velocity higher at autumn than at spring equinox in the longitude range from 320° to 150°, and the opposite occurred at other longitudes.

The EA in the ionosphere also involves the asymmetry in the chemical and dynamical processes. The equinoctial differences in hmF2 cannot fully explain EA in NmF2. For example in noontime, the equinoctial difference of hmF2 is weaker/moderate in LSA/HSA but the EA in NmF2 is stronger/weaker in LSA/HSA respectively. The asymmetry existing in neutral density may also contribute to NmF2 as found by Liu et al. (2007) at 400 km and mass densities were higher in March (about 7–10%) than in September during high-solar activity (F10.7 = 150 sfu) where atomic oxygen dominated at the F2 layer altitudes. As at the F2 peak altitude, both photochemical processes and dynamics processes are significant hence the thermospheric composition may also play an important role for EA in NmF2. We found O/N_2 using the MSIS model more or less different around March (higher) than around the September (not shown as separate Figure) throughout the day as previously also reported by Balan et al. (1997, 1998) and Aggarwal et al. (2012). So the potential equinoctial difference in O/N_2 could also be one of a reason for the EA of the NmF2 presented in this paper. The increased neutral density (without O/N_2 changing) also results in higher electron density (Ne) at low latitudes (Chen et al., 2009) and hence the equinoctial differences of neutral density also affects the EA in the Ne. It is to be noted that the EA in neutral density and Ne in EIA trough as well as crest regions, enhances the EA induced by the difference of the $E \times B$ vertical drift in one region (EIA trough or crest region) while weakens it in the other region which also causes the observed EA at low latitudes (Chen et al., 2009). We examined the relation of the existing background neutral atmosphere (O, O_2, N_2, O/O_2, O/N_2 and mass densities) with the NmF2 and hmF2 as the existing neutral composition of thermosphere may also play a role in causing EA as previously reported by Dasgupta et al. (1983). Sato et al. (1989) assumed ions as oxygen ions, O^+ except in the region below 270 km altitude, where a combination of O^+, NO^+, and O_2^+ ions were assumed, but the molecular ions becomes important only below about 230 km altitude. Our COSMIC observations for hmF2 varies between 215 and 500 km throughout the day (Fig. 4). In the morning, the F-layer comes down to lower altitudes where contribution of neutrals may also be significant. The observed different behaviour in equinoxes may not be only affected by the solar activity as the mean solar activity indices (F10.7P) is nearly same (with slightly higher/lower in LSA/HSA in vernal) in all years except year 2013 (Fig. 1). Our observations exhibited a clear solar activity dependence (both F10.7 and EUV) of NmF2 (strong correlation, 0.8–1.0) throughout the day for both the equinoxes and latitudinal regions respectively (Figs. 3 and 5). These observations are also in agreement to the previous investigators. Oliver et al. (2008) also found the solar activity dependence of NmF2 at mid latitudes as mainly due to the change of solar EUV intensity and considered secondarily due to the changes of neutral composition at the base of the thermosphere. Liu et al. (2003) found a saturation effect in the variation of NmF2 with solar EUV flux and confirmed that it cannot only be attributed to the nonlinear increase of EUV flux with F10.7 but the dynamic processes and neutral atmosphere variability should also play a significant role. During our study period, NmF2 is found unrelated (<0.35) with Kp at all times but moderate-inversely correlated (~0.5–0.7) with Dst in autumn throughout the day (Fig. 5) indicating a stronger role of hourly geomagnetic activity and electric fields in the autumn equinoxes. Wu et al. (2004) also found strength of crest (Ic) not well correlated with Kp index ($r = 0.41$) but strongly associated with Dst index ($r = 0.72$) during the solar minimum near Taiwan and suggested Dst a more suitable parameter for studying long-term ionospheric dynamics around the EIA regions. Aggarwal et al. (2012) also found a moderate relation of strength of ionization anomaly crest, Ic with Dst (0.35) whereas no relation existed with the Kp.

During nighttime, we found EA to be weaker/stronger in NmF2 during LSA/HSA and stronger in hmF2 for both solar activities. The neutral densities (O, O_2, N_2 and mass-densities) are lower and the ratios (O/N_2 and O/O_2) are higher in vernal compared to autumn in nighttime exhibiting EA in neutral compositions (not shown as separate Figure). The distinct correlation existed for neutrals (O, O_2, N_2, mass-densities and O/N_2) with NmF2 and O, O_2, N_2 and mass-densities with hmF2 in the equinoxes during nighttime which may play a role in the EA. During morning hours, similar behaviour of EA in NmF2 as in nighttime is observed but EA for morning hmF2 is weaker in both solar activities. During noontime, EA in NmF2 existed in both solar activities (strong/weak in LSA/HSA) and weak/strong in hmF2 during LSA/HSA respectively. The different densities of O, O_2, N_2 and mass density varying with solar activity and a lower/higher in LSA/HSA in vernal and reversed behaviour of O/O_2 in equinoxes is observed. The O/N_2 is found to be high for all years in vernal. Though all neutrals are strongly coupled to both NmF2 and hmF2 in noontime and are not distinct in the equinoxes indicating a minor role of neutrals and suggest that other factors like F10.7P, EEJ, meridional winds being a major contributor for noontime EA. Aggarwal et al. (2012) found that all parameters (F10.7, EUV, Dst, EEJ, O/N_2) plays a moderate role in EA in daytime anomaly crest (Ic) for all seasons but the O/N_2 plays a major dominant role in spring equinox during noontime. They found that though EEJ and O/N_2 values were higher in autumn but still the Ic was higher in spring and was due to a stronger association of Ic with EEJ in spring (0.69) than autumn (0.5) equinox respectively. We found stronger/moderate correlation of NmF2 with O/N_2 in vernal/autumn in nighttime respectively (Fig. 5). The NmF2 is also found to be strongly correlated with molecular densities O/O_2 (0.64–0.96) but are not distinct in equinoxes throughout the day. Overall, the correlations with other parameters are also higher during vernal compared to autumn and hence the contributions of neutrals cannot be ignored specially in the nighttime. Another possible reason for the EA could be the thermospheric neutral winds which may also transport the electron density to the EIA crest region, depending upon the direction and strength of the wind. However, since we do not have an estimate of thermospheric winds, the proposed mechanism cannot be fully validated, but is a possibility.

The asymmetry near the peak and above is considered to be through the dynamical processes which involve neutral winds and electric fields (Balan et al., 2000; Aggarwal et al., 2012). During noontime/mid-nighttime the F-layer is at higher/lower altitude (hmF2). Balan et al. (1997, 2000) found the altitudinal dependence of daytime (1000–1600 LT) electron density (Ne) being higher/lower in September than March in lower/higher altitudes respectively. The asymmetry in thermospheric composition was accounted for the bottomside ionosphere whereas the stronger EA (higher Ne in March) near and above F-peak is accounted for the weaker daytime poleward wind (at 300 km) in March compared to September which resulted in a broader ionosphere with a peak at higher higher/lower altitude in March/September equinox respectively. This difference in the neutral winds in the topside with minor contribution from the asymmetry in the plasma drifts were accounted for the asymmetry in Ne at higher altitudes. Similar observations were found by Kawamura et al. (2002) and suggested the EA in the neutral wind velocity to be due to the possible differences in the momentum/energy being transmitted from lower to upper atmosphere through tides and waves. Another factor other than composition and wind velocity changes is the equatorial fountain effect which also modifies the ionization profile near the anomaly crest region.

4. Summary

The observed characteristics of ionospheric parameters: NmF2 and hmF2 over Indian longitudinal sector (5–30° N geog. lat., 60–100° E geog. long.) using COSMIC measurements are summarized here:

NmF2:

(a) Diurnal trend exhibits a clear solar activity dependence in noontime and an evening/post-midnight enhancement for both regions and equinoxes respectively.
(b) Day-to-day variability (CV) is lower during daytime but higher in nighttime and early morning hours irrespective of solar activities.
(c) A weaker/stronger EA occurs during nighttime and morning in LSA/HSA and stronger/weaker in noontime in low-/high-solar activity period respectively.
(d) The solar activity indices exhibits a strong positive correlation with NmF2 throughout the day and NmF2 is independant of Kp in both equinoxes and Dst in vernal over equatorial-low latitudes. The NmF2 is weakly related with O and mass densities in nighttime but inversely moderate-strongly related at other times of day. The molecular neutral densities: O_2, N_2 and O/N_2 are highly correlated with NmF2 for both equinoxes and regions throughout the day (except nighttime over equator in vernal, O_2, N_2 and O/N_2 and low-latitude in autumn, N_2, O/N_2) respectively. Whereas O/O_2 plays a significant role throughout the day in NmF2.

hmF2:

(a) Diurnal trend exhibits maxima (noontime, evening/midnight) and minima (early-morning, before-evening/before-midnight) with a strong solar-activity dependence during morning and noontime (higher over equator) and a secondary peak in evening/midnight occurs over equator during HSA/LSA respectively.
(b) The CV over equator is higher during early morning and nighttime in autumn for all years whereas over low latitude, is lower/higher in LSA/HSA for both the equinoxes and is higher in noontime-autumn (except 2011) respectively.
(c) A stronger EA occurs in nighttime for all years and weaker in morning over both regions with stronger in HSA during noontime.
(d) The solar indices are strongly correlated for the whole day and Kp and Dst plays no role in vernal but the Dst strongly correlates in autumn. The hmF2 strongly anti-couples with O, N_2 and mass densities throughout the day for both regions except a weak relation for vernal over equator and autumn over low-latitude in nighttime respectively. A strong relation is found of O_2 (inversely), O/N_2 and O/O_2 (directly) throughout the day.

Some of our reported results using COSMIC observations are in agreement with previous findings using ground based ionosonde measurements for the Indian longitudinal sector. We found the EA in NmF2 is not just a daytime phenomenon but also occurs in nighttime during the high solar activity. The different equinoctial behaviour in hmF2 is also observed in nighttime for both solar activities and in noontime during high solar activity respectively. The results also give a viewpoint for the development of model. Thus, although EA observed in the ionosphere has been interpreted in terms of the combined effect of the corresponding asymmetry in thermospheric composition and solar flux, the basic cause of the asymmetry in the ionosphere is unknown. It should be pointed out here that this work of examining the ionospheric variability using COSMIC during equinoxes is not enough to reveal all the characteristics of ionospheric variability. Hence more studies are planned for the near future using ground and satellite based measurements.

Acknowledgement

MA is grateful to the Department of Science and Technology (DST)-SERB, India for awarding the Ramanujan Fellowship during the study period. She is also grateful to Prof. D.S. Ramesh, Director of IIG, Mumbai for providing the hosting facilities at the Institute. The data has been obtained by OMNI website for geomagnetic and interplanetary parameters, the CELIAS/SEM experiment on SOHO spacecraft for EUV fluxes, COSMIC measurements (http://www.cosmic.ucar.edu/) and the neutral atmosphere by MSISE-00 model (http://ccmc.gsfc.nasa.gov/modelweb/atmos/nrlmsise00.html) are highly acknowledged for making the data available online. We are grateful to the Editor and Potential Reviewers whose constructive comments and suggestions have made us to improve the results.

References

Abdu, M.A., Walker, G.O., Reddy, B.M., Sobral, J.H.A., Fejer, B.G., Kikuchi, T., Trivedi, N.B., Szuszczewicz, E.P., 1990. Electric field versus neutral wind control of the equatorial anomaly under quiet and disturbed condition: a global perspective from SUNDIAL 86. Ann. Geophys. 8, 419–430.

Abdu, M.A., Batista, I.S., Walker, G.O., Sobral, J.H.A., Trivedi, N.B., de Paula, E.R., 1995. Equatorial ionospheric electric fields during magnetospheric disturbances: local time/longitude dependences from recent EITS campaigns. J. Atmos. Terres. Phys. 57, 1065–1083.

Abdu, M.A., 1997. Major phenomena of the equatorial ionosphere-thermosphere system under disturbed conditions. J. Atmosp. Terres. Phys. 59, 1505–1519.

Abdu, M.A., Ramkumar, T.K., Batista, I.S., Brum, C.G.M., Takahashi, H., Reinisch, B.W., Sobral, J.H.A., 2006. Planetary wave signatures in the equatorial atmosphere ionosphere system, and mesosphere- E- and F-region coupling. J. Atmos. Sol.-Terres. Phys. 68 (3–5), 509–522.

Abdu, M.A., Batista, I.S., Brum, C.G.M., MacDougall, J.W., Santos, A. M., de Souza, J.R., Sobral, J.H.A., 2010. Solar flux effects on the equatorial evening vertical drift and meridional winds over Brazil: a comparison between observational data and the IRI model and the HWM representations. Adv. Space Res. 46 (8), 1078–1085.

Aggarwal, M., Joshi, H.P., Iyer, K.N., 2007. Solar activity dependence of electron and ion temperatures using SROSS C2 RPA data and comparison with IRI model. J. Atmos. Terr. Phys. 69, 860–874.

Aggarwal, M., Joshi, H.P., Iyer, K.N., Kwak, Y.-S., Lee, J.J., Chandra, H., Cho, K.S., 2012. Day-to-day variability of equatorial anomaly in GPS-TEC during low solar activity period. Adv. Space Res. 49 (12), 1709–1720.

Aggarwal, M., Joshi, H.P., Iyer, K.N., Kwak, Y.S., 2013. Response of the EIA ionosphere to the 7–8 May 2005 geomagnetic storm. Adv. Space Res. 52 (4), 591–603.

Aggarwal, M., 2015. Anomalous changes in ionospheric TEC during an earthquake event of 13–14 April 2010 in the Chinese sector. Adv. Space Res. 56 (7), 1400–1412.

Akala, A.O., Adeloye, A.B., Somoye, E.O, 2010. Ionospheric foF2 variability over the Southeast Asian sector. J. Geophys. Res., 115, A9, CiteID A09329.

Aravindan, P., Iyer, K.N., 1990. Day to day variability in ionospheric electron content at low latitudes. Planet. Space Sci. 38, 743–750.

Bailey, G.J., Su, Y.Z., Oyama, K.-I., 2000. Yearly variations in the low-latitude topside ionosphere. Ann. Geophys. 18 (7), 789–798.

Balan, N., Otsuka, Y., Fukao, S., 1997. New aspects in the annual variation of the ionosphere observed by the MU Radar. Geophys. Res Lett. 24 (18), 2287–2290.

Balan, N., Otsuka, Y., Bailey, G.J., Fukao, S., 1998. Equinoctial asymmetries in the ionosphere and thermosphere observed by the MU radar. J. Geophys. Res. 103 (A5), 9481–9496.

Balan, N., Otsuka, Y., Fukao, S., Abdu, M.A., Bailey, G.J., 2000. Annual variations of the ionosphere: a review based on MU radar observations. Adv. Space Res. 25, 153–162.

Bardhan, A., Aggarwal, M., Sharma, D.K., Rai, J., 2014. Equinoctial asymmetry in low latitude ionosphere as observed by SROSS-C2 satellite. J. Atmos. Sol.-Terres. Phys. 117, 101–109.

Basu, S., Groves, K.M., Basu, Su., Sultan, P.J., 2002. Specification and forecasting of scintillations in communication/navigation links: current status and future plans. J. Atmos. Sol.-Terres. Phys. 64 (16), 1745–1754.

Batista, I.S., Abdu, M.A., de Medeiros, R.T., de Paula, E.R., 1996. Comparison between IRI predictions and digisonde measurements at low latitude station. Adv. Space Res. 18 (6), 49–52.

Bilitza, D., Obrou, O.K., Adeniyi, J.O., Oladipo, O., 2004. Variability of f_oF2 in the equatorial ionosphere. Adv. in Space Res. 34 (9), 1901–1906.

Chakraborty, S.K., Hajra, R., 2008. Solar control of ambient ionization of the ionosphere near the crest of the equatorial anomaly in the Indian zone. Ann. Geophys. 26 (1), 47–57.

Chapman, S., 1931. The absorption and dissociative or ionizing effect of monochromatic radiation in an atmosphere on a rotating Earth-II, Grazing incidence, Proc. phys. Soc., 43, 483–501 (London).

Chen, Y., Liu, L., Wan, W., Yue, X., Su, S. Y., 2009. Solar activity dependence of the topside ionosphere at low latitudes. J. Geophys. Res., 114, A8, CiteID A08306.

Chen, Y., Liu, L., 2010. Further study on the solar activity variation of daytime $N_m F_2$. J. Geophys. Res. 115, A12337. http://dx.doi.org/10.1029/2010JA015847.

Chen, Y., Liu, L., Wan, W., Ren, Z., 2012. Equinoctial asymmetry in solar activity variations of NmF2 and TEC. Ann. Geophys. 30 (3), 613–622.

Chu, Y.H., Wu, K.H., Su, C.L., 2010. Reply to comment by J. Lei et al. on "A new aspect of ionospheric E region electron density morphology". J. Geophys. Res., 115, A07314, http://dx.doi.org/10.1029/2010JA01.

Chuo, Y.J., Lee, C.C., 2008. Ionospheric variability at Taiwan low latitude station: comparison between observations and IRI-2001 model. Adv. Space Res. 42 (4), 673–681. http://dx.doi.org/10.1016/j.asr.2007.04.

Croom, S.A., Robbins, A.R., Thomas, J.O., 1960. Nature 184, 902.

Da Rosa, A.V., Waldman, H., Bendito, J., Garriott, O.K., 1973. Response of the ionospheric electron content to fluctuations in solar activity. J. Atmos. Terr. Phys. 35, 1429–1442.

DasGupta, A., Basu, S., Aarons, J., Klobuchar, J.A., Basu, S., Bushby, A., 1983. VHF amplitude scintillations and associated electron content depletions as observed at Arequipa, Peru. J. Atmos. Terr. Phys. 45, 15.

Davies, K., 1990. Ionospheric Radio. Peter Peregrinus, London.

Ezquer, R.G., Mosert, M., 2007. Ionospheric variability studies in Argentina. Adv. Space Res. 39 (5), 949–961.

Fejer, B.G., Gonzalez, S.A., de Paula, E.R., Woodman, R.F., 1991. Average vertical and zonal F region plasma drifts over Jicamarca. J. Geophys. Res., 96, 13, 901–13, 906.

Fejer, B.G., Scherliess, L., 1997. Empirical models of storm time equatorial zonal electric fields. J. Geophys. Res., 102.24, 047–24,056.

Fejer, B.G., Jensen, J.W., Su, S.Y., 2008. Seasonal and longitudinal dependence of equatorial disturbance vertical plasma drifts. Geophys. Res. Lett. 35, L20106. http://dx.doi.org/10.1029/2008GL035584.

Feynman, J., Gabriel, S.B., 2000. On space weather consequences and predictions. J. Geophys. Res., 105 (A5), 10,543, http://dx.doi.org/10.1029/1999JA000141.

Fuller-Rowell, T.J., Rees, D., Quegan, S., Moffett, R.J., Bailey, G.J., 1988. Simulations of the seasonal and universal time variations of the high-latitude thermosphere and ionosphere using a coupled, three-dimensional model. Pure Appl. Geophys. 127, 189–217. http://dx.doi.org/10.1007/BF0087981.

Hanson, W.B., Patterson, T.N.L., 1964. Planet. Space Sci. 12, 979.

Hargreaves, J.K., 1995. The Solar-Terrestrial Environment: An Introduction to Geospace—The Science of the Terrestrial Upper Atmosphere, Ionosphere, and Magnetosphere, Cambridge Atmos. Space Sci. Ser., 5, Cambridge Univ. Press., New York.

Hu, L., Ning, B., Liu, L., Zhao, B., Li, G., Wu, B., Huang, Z., Hao, X., Chang, S., Wu, Z., 2014. Validation of COSMIC ionospheric peak parameters by the measurements of an ionosonde chain in China. Ann. Geophys. 32 (10), 1311–1319.

Huang, Y.-N., Cheng, K., 1996. Solar cycle variations of the equatorial ionospheric anomaly in total electron content in Asian region. J. Geophys. Res. 101 (A11), 24513–24520.

Ivanov-Kholodny, G.S., Mikhailov, A.V., 1986. The Prediction of Ionospheric Conditions, 167. Springer, New York.

Judge, D.L., McMullin, D.R., Ogawa, S., Hovestadt, D., Klecker, B., Hilchenbach, M., Canfield, L.R., Vest, R.E., Watts, R., Tarrio, C., Kuhne, M., Wurz, P., 1998. First solar EUV irradiances obtained from SOHO by the CELIAS/SEM. Sol. Phys. 177, 161–173.

Kalita, B.R., Bhuyan, P.K., 2017. Variations of the ionospheric parameters and vertical electron density distribution at the northern edge of the EIA from 2010 to 2015 along 95E and comparison with the IRI-2012, Adv. Space Res. 60 (2), 295–306, http://dx.doi.org/10.1016/j.asr.2016.06.041.

Kawamura, S., Balan, N., Otsuka, Y., Fukao, S., 2002. Annual and semiannual variations of the midlatitude ionosphere under low solar activity. J. Geophys. Res. 107, A81166. http://dx.doi.org/10.1029/2001JA000267.

Kohl, H., King, J.W., 1967. Atmospheric winds between 100 and 700 km and their effects on the ionosphere. J. Atmos. Terr. Phys. 29, 1045–1062.

Krankowski, A., Zakharenkova, I., Krypiak-Gregorczyk, A., Shagimuratov, I., Wielgosz, P., 2011. Ionospheric electron density observed by FORMOSAT-3/COSMIC over the European region and validated by ionosonde data. J. Geod. 85 (12), 949–964. http://dx.doi.org/10.1007/s00190-011-0481-z.

Kumar, S., Singh, R.P., Tan, E.L., Singh, A.K., Ghodpage, R.N., Siingh, D., 2016. Temporal and spatial deviation in F2 peak parameters derived from FORMOSAT-3/COSMIC. Space Weather 14 (6), 391–405.

Kuo, Y.-H., Wee, T.-K., Sokolovskij, S., Rocken, C., Schreiner, W., Hunt, D., Anthes, R.A., 2004. Inversion and error estimation of GPS radio occultation data. J. Meteorol. Soc. Japan 82 (1B), 507–531.

Liu, J.Y., Chen, Y.I., Lin, J.S., 2003. Statistical investigation of the saturation effect in the ionospheric foF2 versus sunspot, solar radio noise, and solar EUV radiation. J. Geophys. Res. 108 (A2), 1067. http://dx.doi.org/10.1029/2001JA007543.

Liu, L., Wan, W., Ning, B., Pirog, O.M., Kurkin, V.I., 2006. Solar activity variations of the ionospheric peak electron density. J. Geophys. Res. 111, A08304. http://dx.doi.org/10.1029/2006JA011598.

Liu, L., Zhao, B., Wan, W., Venkartraman, S., Zhang, M.-L., Yue, X., 2007. Yearly variations of global plasma densities in the topside ionosphere at middle and low latitudes. J. Geophys. Res. 112, A07303. http://dx.doi.org/10.1029/2007JA012283.

Liu, L., Zhao, B., Wan, W., Ning, B., Zhang, M.L., He, M., 2009. Seasonal variations of the ionospheric electron densities retrieved from Constellation Observing System for Meteorology, Ionosphere, and Climate mission radio occultation measurements. J. Geophys. Res. 114, A02302. http://dx.doi.org/10.1029/2008JA013.

Liu, L., He, M., Yue, X., Ning, B., Wan, W., 2010a. Ionosphere around equinoxes during low solar activity. J. Geophys. Res. 115, A09307. http://dx.doi.org/10.1029/2010JA015318.

Liu, J.-Y., Lee, C.C., Yang, J.Y., Chen, C.Y., Reinisch, B.W., 2010b. Electron density profiles in the equatorial ionosphere observed by the FORMOSAT-3/COSMIC and a digisonde at Jicamarca. GPS Solut. 14, 75–81. http://dx.doi.org/10.1007/s10291-009-0150-3.

Liu, L., Le, H., Chen, Y., He, M., Wan, W., Yue, X., 2011. Features of the middle- and low-latitude ionosphere during solar minimum as revealed from COSMIC radio occultation measurements. J. of Geophys. Res. 116, A09307. http://dx.doi.org/10.1029/2011JA016691.

Maruyama, T., Saito, S., Kawamura, M., Nozaki, K., Krall, J., Huba, J. D., 2009. Equinoctial asymmetry of a low-latitude ionosphere-thermosphere system and equatorial irregularities: evidence for meridional wind control. Ann. Geophys. 27, 2027–2034.

Miller, K.L., Tort, D.G., Richards, P.G., 1986. Meridional winds in the thermosphere derived from measurement of F2 layer height. J. Geophys. Res. 91, 4531–4535.

Miller, C.A., Swartz, W.E., Kelley, M.C., Mendillo, M., Nottingham, D., Scali, J., Reinisch, B., 1997. Electrodynamics of midlatitude spread F, 1. Observations of unstable, gravity wave-induced ionospheric electric fields at tropical latitudes. J. Geophys. Res. 102:11, 521–11,532.

Oliver, W.L., Kawamura, S., Fukao, S., 2008. The causes of the mid-latitude F layer behavior. J. Geophys. Res. 113, A08310. http://dx.doi.org/10.1029/2007JA01259.

Pavlov, A.V., Pavlova, N.M., 2005. Causes of the mid-latitude NmF2 winter anomaly at solar maximum. J. Atmos. Sol.-Terres. Phys. 67 (10), 862–877.

Rama Rao, P.V.S., Niranjan, K., Prasad, D.S.V.V.D., Gopi Krishna, S., Uma, G., 2006. On the validity of the ionospheric pierce point (IPP) altitude of 350km in the Indian equatorial and low-latitude sector. Ann. Geophys. 24, 2159–2168.

Ren, Z., Wan, W., Liu, L., Chen, Y., Le, H., 2011. Equinoctial asymmetry of ionospheric vertical plasma drifts and its effect on F-region plasma density. J. Geophys. Res. 116, A02308. http://dx.doi.org/10.1029/2010JA016081.

Richards, P.G., Torr, D.G., 1986. A factor of 2 reduction in the theoretical F2 peak electron density due to enhanced vibrational excitation of N2 in summer at solar maximum. J. Geophys. Res. 91 (11), 11331–11336.

Richards, P., Fennelly, J., Torr, D., 1994a. EUVAC: a solar EUV flux model for aeronomic calculations. J. Geophys. Res. 99, 8981–8992.

Richards, P., Fennelly, J., Torr, D., 1994b. Correction to "EUVAC: a solar EUV flux model for aeronomic calculations". J. Geophys. Res. 99, 13283.

Rishbeth, H., 1972. Thermospheric winds and the F-region: a review. J. Atmos. Terr. Phys. 34, 1–47.

Rishbeth, H., 2000. The equatorial F-layer: progress and puzzles. Ann. Geophys. 18, 730–739. http://dx.doi.org/10.1007/s00585-000-0730-6.

Rishbeth, H., Garriott, O.K., 1969. Introduction to Ionospheric Physics. International Geophysics Series, vol. 14. Academic Press, New York.

Rishbeth, H., Müller-Wodarg, I.C.F., Zou, L., Fuller-Rowell, T.J., Millward, G.H., Moffett, R.J., Idenden, D.W., Aylward, A.D., 2000. Annual and semiannual variations in the ionospheric F2-layer: II. Physical discussion. Ann. Geophys. 18, 945–956. http://dx.doi.org/10.1007/s00585-000-0945-6.

Sato, T., Ito, A., Oliver, W.L., Fukao, S., Tsuda, T., Kato, S., Kimura, I., 1989. Ionosphere incoherent scatter measurements with the MU radar: techniques and capability. Radio Sci. 24, 85–98.

Scherliess, L., Fejer, B.G., 1999. Radar and satellite global equatorial F region vertical drift model. J. Geophys. Res. 104 (A4). http://dx.doi.org/10.1029/1999JA900025.

Schreiner, W.S., Sokolovskiy, S.V., Rocken, C., Hunt, D.C., 1999. Analysis and validation of GPS/MET radio occultation data in the ionosphere. Radio Sci. 34 (4), 949–966.

Sethi, N.K., Dabas, R.S., Vohra, V.K., 2004. Diurnal and seasonal variations of hmF2 deduced from digital ionosonde over New Delhi and its comparison with IRI-2001. Ann. Geophys. 22, 453–458.

Sharma, D.K., Rai, J., Israil, M., Subrahmanyam, P., 2005. Diurnal, seasonal and latitudinal variation of ionospheric temperatures of the topside F region over Indian region during solar minimum year 1995–96. J. Atmos. Sol.-Terr. Phys. 67, 269–274.

Straus, P.R., 2007. Ionospheric climatology derived from GPS occultation observations made by the ionospheric occultation experiment. Adv. Space Res. 39, 793–802.

Syndergaard, S., Schreiner, W.S., Rocken, C., Hunt, D.C., Dymond, K. F., 2006. Preparing for COSMIC: inversion and analysis of ionospheric data products. In: Foelsche, U., Kirchengast, G., Steiner, A.K. (Eds.), Atmosphere and Climate: Studies by Occultation Methods. Springer-Verlag, Berlin, pp. 137–146.

Titheridge, J.E., 1973. The electron content of the southern mid-latitude ionosphere 1965–1971. J. Atmos. Terr. Phys. 35, 981–1001.

Tobiska, W.K., Woods, T., Eparvier, F., Viereck, R., Floyd, L., Bouwer, D., Rottman, G., White, O.R., 2000. The Solar 2000 empirical solar irradiance model and forecast toll. J. Atmos. Sol. Terr. Phys. 62, 1233–1250.

Tsai, L.C., Tsai, W.H., Schreiner, W.S., Berkey, F.T., Liu, J.Y., 2001. Comparisons of GPS/MET retrieved ionospheric electron density and ground based ionosonde data. Earth Planets Space 53, 193–205.

Tsai, L.C., Tsai, W.H., 2004. Improvement of GPS/MET ionospheric profiling and validation using the Chung-Li IONOSONDE measurements and the IRI model. Terr. Atmos. Ocean Sci. 15, 589–607.

Unnikrishnan, K., Nair, R.B., Venugopal, C., 2002. A comparative study of night time enhancement of TEC at a low latitude station on storm and quiet nights including the local time, seasonal and solar activity dependence. Ann. Geophys. 20, 1843–1850.

Wan, W., Liu, L., Pi, X., Zhang, M.L., Ning, B., Xiong, J., Ding, F., 2008. Wavenumber-4 patterns of the total electron content over the low latitude ionosphere. Geophys. Res. Lett. 35, L12104. http://dx.doi.org/10.1029/ 2008GL0337.

Woodman, R.F., La Hoz, C., 1976. Radar observations of F region equatorial irregularities. J. Geophys. Res. 81, 5447–5466.

Wu, C.C., Fry, C.D., Liu, J.Y., Liou, K., Tseng, C.L., 2004. Annual TEC variation in the equatorial anomaly region during the solar minimum: September 1996–August 1997. J. Atmos. Sol. Terr. Phys. 66, 199–207.

Wu, X., Hu, X., Gong, X., Zhang, X., Wang, X., 2009. An asymmetry correction method for ionospheric radio occultation. J. Geophys. Res. 114, A03304. http://dx.doi.org/10.1029/2008JA013025.

Yue, X., Schreiner, W.S., Lei, J., Sokolovskiy, S.V., Rocken, C., Hunt, D. C., Kuo, Y.-H., 2010. Error analysis of Abel retrieved electron density profiles from radio occultation measurements. Ann. Geophys. 28, 217–222.

Zhang, S.-R., Holt, J.M., 2008. Ionospheric variability from an incoherent scatter radar long-duration experiment at Millstone Hill. J. Geophys. Res. 113, A03310. http://dx.doi.org/10.1029/2007JA012639.